Applied Physics Research; Vol. 16, No. 1; 2024
ISSN 1916-9639 E-ISSN 1916-9647
Published by Canadian Center of Science and Education

Simple Estimation of the Trapping Height in Optical Tweezers

Abad ê Ange-Boris N'guessan[1], Pavel Yale[1], Edoukoua Jean Michel Konin[1,2] & Michel Abaka Kouacou[1]

[1] Laboratoire d'Instrumentation, Image et Spectroscopie (L2IS), Institut National Polytechnique, Félix Houphou ët-Boigny (INPHB), BP 1093 Yamoussoukro, Côte d'Ivoire

[2] Université Alassane Ouattara, Bouaké, Côte d'Ivoire

Correspondance: Abad ê Ange-Boris N'guessan, Laboratoire d'Instrumentation Image et Spectroscopie, Unité Mixte de Recherche et d'Innovation en Electronique et Electricit é Appliqu ée, Institut National Polytechnique Houphouët Boigny BP 1093 Yamoussoukro, Côte d'Ivoire. E-mail: abade.nguessan19@inphb.ci

Received: March 24, 2023 Accepted: May 28, 2023 Online Published: February 7, 2024

doi:10.5539/apr.v16n1p10 URL: https://doi.org/10.5539/apr.v16n1p10

Abstract

The trapping height is an important quantity that influences the parameters measured by optical tweezers such as the stiffness, the force and stability of the trap. In this paper, we propose a simple method using video microscopy and based on tracking of particles positions in the axial and radial directions. The positional fluctuations in the axial direction were used to estimate the trap height and determine the trap stiffness using Boltzmann statistics. This method makes it possible to obtain simultaneously the trap stiffness and the trap height. The entropy values of the information for each image allowed us to validate this method because of the relation which exists between it and the axial displacements. Note that this method is simple and quick to determine the height of the trap if it has not been estimated at the start or during the measurement.

Keywords: optical tweezers, laser power, trap stiffness, trapping height

1. Introduction

The optical tweezers is a technique for measuring very small forces developed in the 1970s by Arthur Ashkin (Ashkin, 1970). From a laser beam strongly focused by a microscope objective with a large aperture on a point in the plane of the sample, a trap is created and allows to manipulate macroscopic particles. Once the trap is created, two types of forces compete namely: the scattering force that pushes the particle along the direction of propagation of the laser beam and the force of gradient that pulls the particle at the location of the highest field intensity and thus represents a restoring force towards the focus of the focusing lens system (Grier, 2003). Thus, the restoring force that holds the particle in a stable position is linear with the displacement, x, so that it can be described by an optical equivalent of Hooke's law $F = kx$. Therefore, force measurements are usually divided into two distinct steps: the determination of the stiffness k, or calibration of the trap, and the measurement of the relative displacement x of the trapped particle (Buosciolo *et al.*, 2004). The forces involved are evaluated as a function of the size of the particle. It has become a very important tool in fields such as medicine, biophysics etc. (Grier, 2003; Michel *et al.*, 2017). However, the measured parameters such as axial displacement, trap stiffness, trapping force and trap efficiency (Verdeny *et al.*, 2011; Yale *et al.*, 2016), depend on the distance between the center of the trap and the glass surface at which the measurements were made due to spherical aberrations (Rohrbach, 2005). This distance is called the trapping height. Thus, the trapping height becomes an important factor to consider in the measurements when using an oil immersion objective. There are two methods to calculate the trapping height (Neuman *et al.*, 2005; Ghislain *et al.*, 1994). The first uses the cutoff frequency of a particle trapped at different positions of the slat relative to a fixed objective. From the viscous drag coefficient as a function of height, we can get the relationship between the height of the trap and the coverslip. But this method is based on the hypothesis that the rigidity of the trap is independent of the height. This is not the case when using an oil immersion objective. The second method uses the observation of an oscillating axial signal of a trapped particle as the glass surface moves away. Oscillations come from interference between the beam and its reflection on the trapped bead. This requires a conversion factor for the moving signals. This takes a long time or sometimes difficult to achieve. This shows that only the QPD detector was used to determine the trapping height. It is also determined manually from a three-axis manual translation table that can be moved with greater accuracy by a piezoelectric controller along these three axes.

From one position to another in the axial direction, the image of the particle is different. To describe the motion of the particle in the axial direction, the Shannon information entropy is used. The entropy value of an image of a trapped bead characterizes the defocusing of the bead from the focus(Bao, Li, Lou, & Wang, 2004; Bao, Li, Lou, Gong, *et al.*, 2005).

As a result of these disadvantages, in this study, we propose a method based on the axial displacements of a trapped particle using video microscopy to estimate the trapping height. This method is simple and does not require a conversion factor beforehand.

2. Materials and Methods

2.1 Experimental Setup

For this study, the scheme of the experimental setup is illustrated in figure (Yale *et al.*, 2018). We used an optical tweezers consisting of a Laser diode (Thorlabs, PL980P33J) with a wavelength λ = 980 nm and coupled to an oil immersion objective (MRP01902, Nikon, Tokyo, Japan) of refractive index N = 1.5 focusing the laser beam to create an optical trap. This lens has a numerical aperture of NA = 1.25 and a magnification of 100 X. The emitted light beam arrives at a telescope to increase the beam coming out of the source and transported through an optical fiber. This will cover the entire rear extent of the lens entry face.

The light beam is emitted and enters a telescope, in order to increase the width of the light beam coming out of the source, and to allow it to cover the entire extent of the entrance face of the lens. It then passes through the high numerical aperture 100 X oil immersion objective which creates a narrow beam size where particles are attracted and trapped.

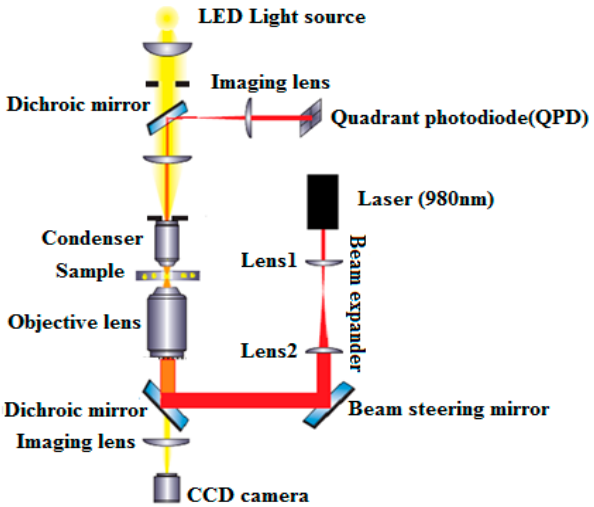

Figure 1. Schematic of the experimental setup (Yale et al., 2018)

This beam passes through the condenser which transforms the strongly divergent beams into parallel rays. The forward scattered light transmitted by the particle is then reflected by a dichroic mirror on the surface of the quadrant photodiode, producing a voltage signal. A white light source (LED) is used to illuminate our sample chamber during the manipulation. The beam then passes through the microscope objective and is guided to the CCD camera equipped with a mirror to eliminate stray reflections from the laser. The camera signal is then sent to a video monitor.

2.2 Sample Preparation

For this manipulation, we used silica beads of 2 µm and 4.5 µm diameter. We introduced 50 µl of the concentrated solution of silica beads into 5000 µl of distilled water.

3. Methods

3.1 Trap Calibration

There are several methods in the literature for determining the trap stiffness k of the trap. In this study, we will focus on the Boltzmann statistics for the calculation of the trap stiffness. Reconstruction of the optical potential

using Boltzmann statistics can be used to determine any continuous trapping landscape in the region accessible by thermal agitation (Osterman, 2010). At equilibrium, the probability density $\rho(\boldsymbol{x})$ of the 1D particle position is given by

$$\rho(x)dx = Cexp\left(\frac{-E(x)}{k_BT}\right) \tag{1}$$

where C is a normalization factor and $E(x)$ is the trapping potential. The shape of $E(x)$ can be obtained from the normalized histogram of the trapped particle positions as follows.

$$E(x) = k_BT(-\ln(\rho(x) + \ln C) \tag{2}$$

The contribution of dx is incorporated into C, the normalization factor, and represented in the second term in equation (2). This term is an energy offset and is neglected assuming a zero potential at the center of the optical trap. To determine the potential energy, the logarithm of the function fitted to the calculated distribution of particle positions is taken and multiplied by $-k_BT$ (Yale *et al.*, 2018). The resulting distribution is fitted by a quadratic equation.

$$E(x) = \frac{1}{2}kx^2 \tag{3}$$

where k is the trap stiffness. Thus:

$$E(x) = \frac{1}{2}kx^2 = -k_BT\ln(\rho(x) \tag{4}$$

$$k = \frac{-2k_BT}{x^2}\ln\big(\rho(x)\big) \tag{5}$$

In the case of the commonly used Gaussian trapping beam $[\mathrm{TEM}]_{00}$, which results in a harmonic trapping potential, one can fit a parabola $y = ax^2 + b$ to the data in the central region of the potential to extract the trap stiffness and check for possible deviations from the perfect harmonic shape. The stiffness coefficient $k = 2a/k_BT$ obtained in this way is more accurate than (3). Another advantage of such a calibration is that it also gives information about the potential in the region away from the center of the trap, where the optical potential is not non-harmonic (Osterman, 2010).

3.2 Methodology of Trapping Height Determination

When a bead is properly trapped, it remains at the same z-position when the stage is moved up and down. This maneuver causes a variation in light intensity in the image of the microbead. It may become slightly blurred due to the change in refraction of the medium. Then the bead can simply be returned to the original z-position for data acquisition. One method of measuring the trapping height is to move the stage upwards once a high intensity is observed within the trapped particle.

Figure 2 illustrates the methodology used in this work. Once the beads were trapped, using a turntable, the trap is moved in the axial direction. This manipulation was carried out at laser power of 57.27 mW, 62.72 mW and 79 mW. The data was acquired with a high-speed (CCD) camera and recorded as video. Once the data was acquired and recorded as video, it was processed and the extraction of the different positions of the microbeads was performed by ImageJ software.

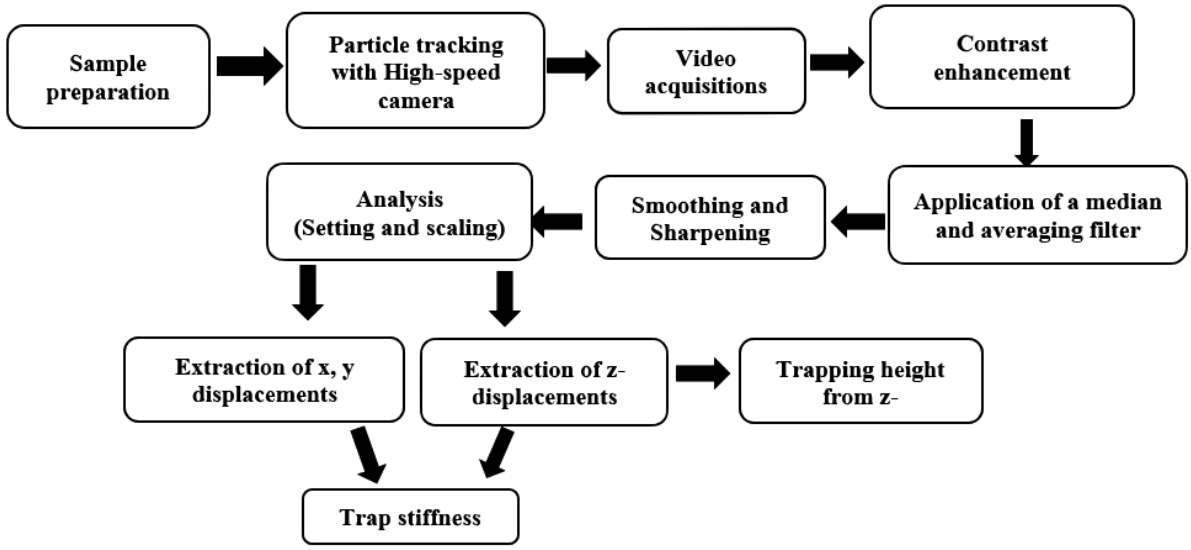

Figure 2. Process for determining the trapping height

The free software Image-J was used to process each image from the recorded video. Figure 3.A shows the initial image of the microbead with less contrast. For this purpose, the videos are processed according to the process shown in Figure 2. Once the video is processed, the different positions occupied by the trapped particle can be extracted and recorded. The relationship between the distances (measured in pixels) and the true measurable distances (in micrometers) must be known before processing the data.

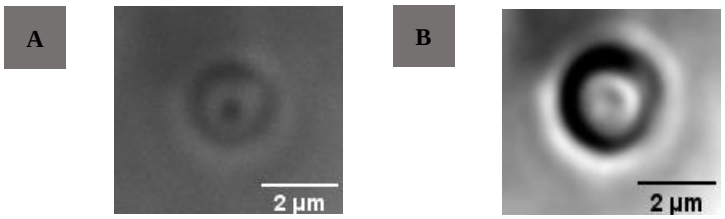

Figure 3. A) Initial image of a silica bead of 2 µm diameter trapped at 57.27 mW; B) Final image after treatment

The positions of the particle in the axial direction are in pixels so it must be converted to µm. For the CCD camera used in this study, the linear relationship between the distance (µm) and the pixels, gives an actual distance which turned out to be $\mathbf{0.0416 \pm \pm 0.0001}\ \mu\boldsymbol{m/pixel}$.

3.3 Information Entropy of a Microbead

Information entropy was initially used to describe the information contained in a message. It then increased and was applied to characterize an image. An image is composed of $j \times k$ pixels, each corresponds to a gray scale. If we assume that there are m pixels with the same gray scale as $i(0 \leq i \leq n)$ where n is the total number of gray scales in the image, the probability with which the gray scale value i appears in the image will be $p_i = \frac{m}{j \times k}$ where $\sum_{i=1}^{n} p_i = 1$. If all p_i are known, the information entropy of the image can be deduced using the following equation

$$H = -\sum_{i=0}^{n} p_i \log(p_i) \tag{6}$$

The image information entropy can characterize a bead and is strictly related to the defocusing of the microbead from the laser focus. It has been used to measure the axial position of a trapped bead (Bao *et al.*, 2004; Bao *et al.*, 2005).

4. Results and Discussions

In this work we varied the laser power at a fixed height and then varied the height for measurements at 57.27 mW, 62.72 mW and 79 mW for beads of 2 μm and 4.5 μm diameter (Figures 4, 5 and 6). After applying our working methodology (Figure 2), the different positions of the particle in the axial and transverse direction were extracted. This allowed us to obtain the typical potential well and the resulting fit are shown in Figure 7.

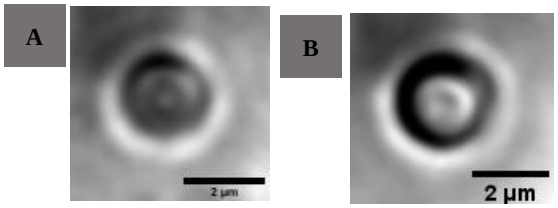

Figure 4. Images of beads of 2 μm diameter trapped at a power of 57.27 mW at different heights $A)\ h = 5.5\ \mu m, B)\ h\ =\ 6\ \mu m$

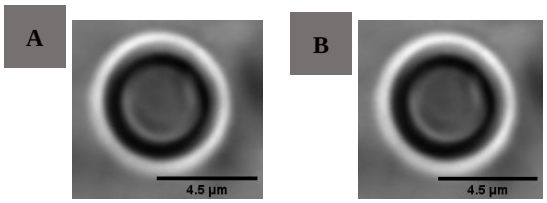

Figure 5. Images of beads of 4.5 μm diameter trapped at a power of 62.72 mW at different heights, $A)\ h = 4.1\ \mu m, B)\ h\ =\ 4.87\ \mu m$

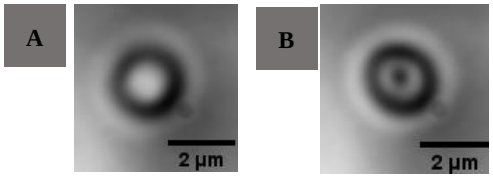

Figure 6. Images of beads of 2 μm diameter trapped at a power of 79 mW at different heights $A)\ h = 5\ \mu m, B)\ h\ =\ 5.8\ \mu m$

Then, the axial and transverse positions were extracted. This allowed us to obtain typical potential well and the resulting fit are shown in Figure 7.

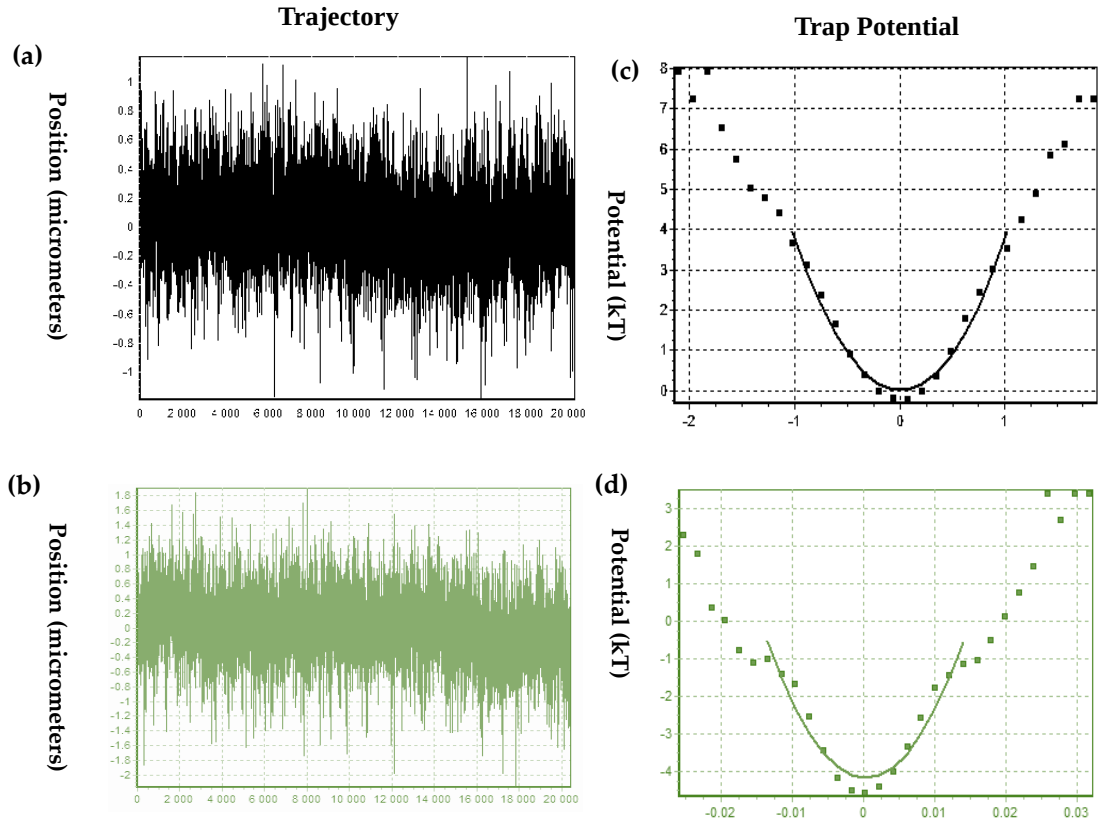

Figure 7. (a) and (c) Trajectory in the axial and transverse direction of a 2 μm diameter microbead, (b) and (d) the potential well resulting from this trajectory and the fit of the 2 μm diameter microbead trapped with a laser power of 57.27 mW

Estimating the trapping height is not as easy because the acquired videos are subject to noise or lack of brightness and contrast. Therefore, careful processing of the videos is essential. After processing the videos, we also used the center of the fluctuations in the axial direction to estimate the trapping height. The yellow line in figure 8 shows the position of the particle at a height of 99.4 pixels.

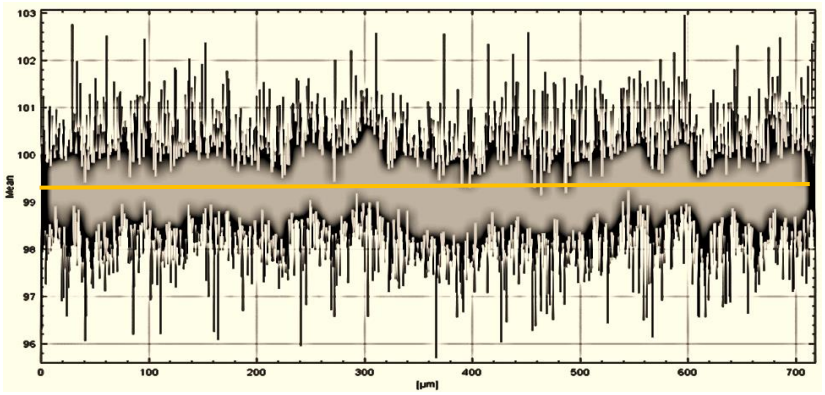

Figure 8. Positional fluctuation of a 4.5 μm diameter silica bead extracted with ImageJ at a laser power of 62.72 mW

Then with the different axial positions, we estimated the height and calculated the trap stiffness. The parameters of the trap are calculated and entered in Table 1:

Table 1. Summary of trap parameters measured in the x, y and z direction for laser power 57.27 mW, 79 mW for the bead for 2 µm and 62.72 mW for 4.5 µm

Laser power (mW)	Height (pixels)	Height (µm)	Trap Stiffness k_x (N/m)	Trap Stiffness k_y (N/m)	Trap Stiffness k_z (N/m)
57.27	132	5.5	$2.27E^{-03}$	$2.60\ E^{-03}$	$1.84E^{-04}$
	144	6	$2.03E^{-03}$	$2.09\ E^{-03}$	$1.37E^{-04}$
62.72	99	4.1	$3.02E^{-03}$	$3.25E^{-03}$	$2.04E^{-04}$
	117	4.87	$2.58E^{-03}$	$2.95\ E^{-03}$	$2.24\ E^{-04}$
79	121	5	$7.96E^{-03}$	$6.83\ E^{-03}$	$3.37\ E^{-04}$
	140	5.8	$6.86E^{-03}$	$5.46\ E^{-03}$	$1.32\ E^{-04}$

We observe that the trap stiffness increases with increasing laser power and decreases with increasing height (Table 1).

The trap stiffness in the transverse and axial direction obtained after the reconstruction of the potential well from this experiment is of the order of $10^{-3}\ N/m$ and $10^{-4}\ N/m$.

The trap stiffness increases with the laser power. The trap stiffness in the transverse direction (x and y) is greater than that in the axial direction (z), i.e, $k_x \approx k_y > k_z$. This shows that our device is well aligned.

Figures 4, 5 and 6 show us the images of trapped beads at different laser power and height above the glass surface. The distribution of the light intensity in the image is a function of the height at which the particle was trapped. Thus, to evaluate the irregularity in these images, we have opted for the calculation of the information entropy of these images. It can be seen as a measure of the uncertainty of an event according to the knowledge we have. It is a value that quantifies this uncertainty. Using equation (6) on Matlab, the entropy of these images has been calculated and listed in Table 2.

Table 2. Entropy values of images of microbeads trapped at different heights at laser power of 57.27 mW, 62.72 mW and 79 mW

57.27 mW		**62.72 mW**		**79 mW**	
Height (µm)	**Entropy**	**Height (µm)**	**Entropy**	**Height (µm)**	**Entropy**
5.5	**7.44**	**4.25**	**6.98**	**5**	**7.12**
6	**7.55**	**4.87**	**7.32**	**5.8**	**7.26**

Entropy values vary with the axial position of the trapped particle. In work (Bao et al., 2005), a 3 µm diameter polystyrene bead adhered to the sample chamber and entropy values decreased with axial position in a linear range. The bead was moved in 10 nm steps and the linearity range is between 2 nm and 9 nm. These values are less than the bead's radius, so the bead hasn't really moved away from the glass surface. In our case, we worked with a 2 µm and 4.5 µm silica bead. In both cases, we find that the entropy values increase as the bead moves away from the glass surface and therefore with increasing axial position and trapping height for our measurements. It is important to mention that the bead does not adhere to the surface of the glass. We can say at steps larger than the radius of the bead, the linear relationship between axial position and entropy is not inverse but increasing.

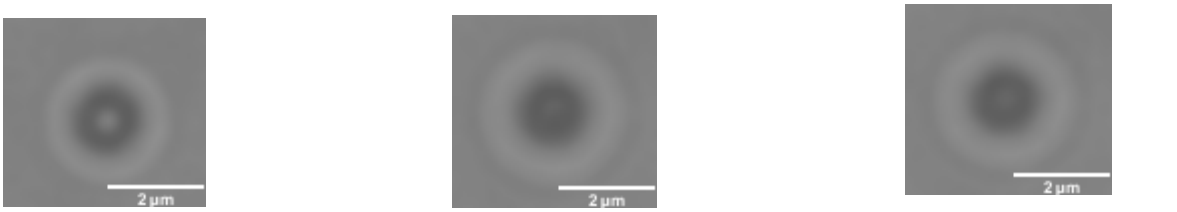

(a) $h = 4.5\ \mu m, H = 4.35$ (b) $h = 5.12\ \mu m, H = 4.50$ (c) $h = 6.04\ \mu m, H = 4.63$

Figure 9. Image of the bead at different positions

Below the pictures, the trapping height and the corresponding information entropy is given.

Figure 9 shows images of a 4.5 µm diameter bead at different trapping heights. The diffusion around the bead becomes stronger when it is on the surface. The plot of the variation of entropy as a function of the trapping height confirms that the increasing relationship (Figure 10.b). This is due to the strong fluctuations of the particles when we trap on the surface, showing that the disorder is high on the surface.

The experimental study between the experimental trapping height determined from our method and the height given by varying the piezoelectric stage with the step of 5 µm in the axial direction, show that there is an increasing linear relationship between the two. Although the proportionality between the two is very small compared to 1, the linearity exists (Figure 10.a).

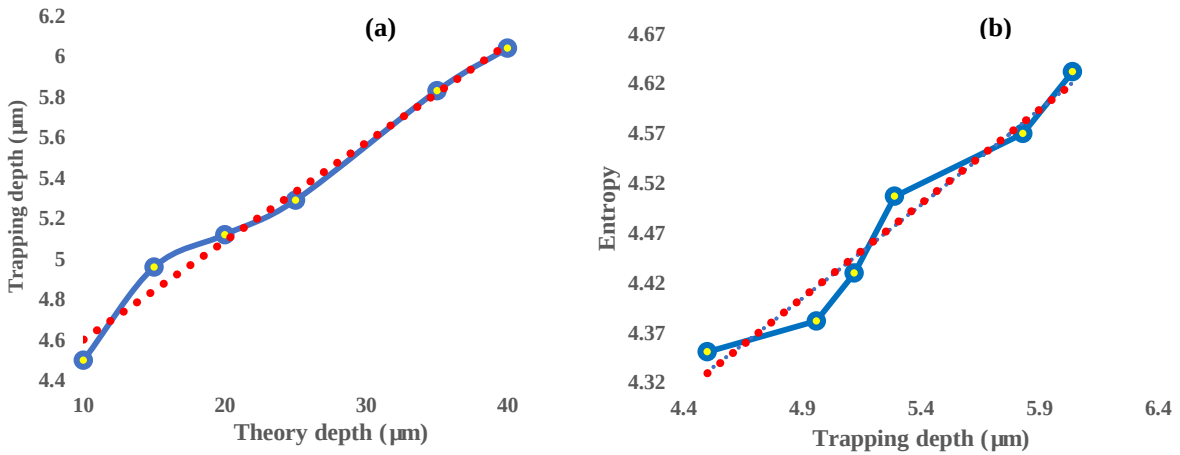

Figure 10. (a) Relationship between trapping height (µm) experimental and theoretical height, (b) Relationship between entropy and trapping height

The radius of the trapped particle in the different acquisitions increases with the trapping height (figure 11). This shows that when the trapping is done on the surface or in depth it has an impact on the size of the particle in the image.

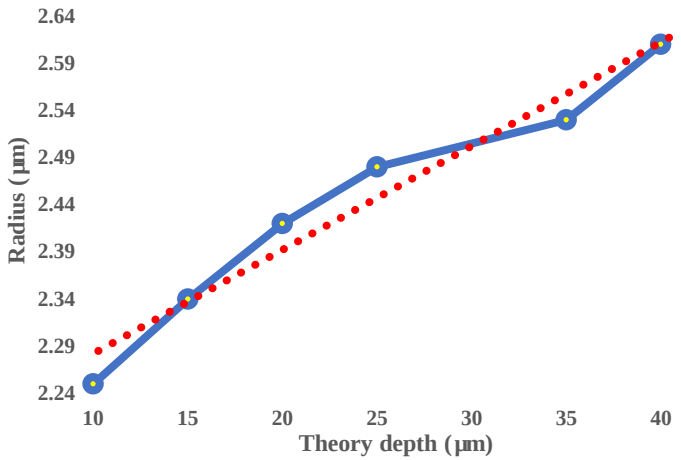

Figure 11. The variation of the bead radius as a function of the trapping height

The radius of the trapped particle in the different acquisitions increases with the height of trapping. This shows that whether the trapping is at the surface or at height it has an impact on the size of the particle in the image. The size of the particle appears larger as the particle moves away from the top glass surface. This is due to the fact that when the particle is trapped on the surface, the scattering around the trapped particle becomes larger. The explanation for this is probably due to the strong fluctuation of the particle when influenced by Brownian motion.

5. Conclusion

The approach, proposed in this study, is based on a simple method of tracking and measuring the positions of the particles. This allowed to determine the height and the trap stiffness for different laser powers. The stiffness showed an inverse linear dependence on the height. This method allows the trap height to be determined without prior knowledge of the initial particle position when the particle is on the lamella. The different values of the entropy of the image information also made it possible to know whether the particle is moving away from the lamella or towards it. This method is simple and can be used by specialists and even non-specialists of the optical tweezers.

However, if the noise in the data and images is under or over estimated, this may eventually change the pixel, entropy and height values. The entropy being a function that is not assigned a unique value of the axial position of a ball will be modified. Once the type of noise is detected, using the appropriate denoising method, this will give good results. For those containing several types of noise, a combination of several denoising methods can be used. The effect of noise is a parameter that must be taken into account in this study.

Acknowledgments

We would like to sincerely thank ISP (the International Science Program) and TWAS (The World Academy of Sciences) TWAS for funding of our research work.

References

Ashkin, A. (1970). Acceleration and Trapping of Particles by Radiation Pressure. *Physical Review Letters*, *24*(4), 156-159. https://doi.org/10.1103/PhysRevLett.24.156

Bao, J. H., Li, Y. M., Lou, L. R., Gong, Z., Wang, Z., & Wang, H. W. (2005). Information entropy method for measuring the axial displacement of a bead and its application to analyzing the trapping force of optical trap. *Electronic Imaging and Multimedia Technology IV*, *5637*, 305. https://doi.org/10.1117/12.570866

Bao, J. H., Li, Y. M., Lou, L. R., & Wang, Z. (2004). Measurement of the axial displacement with information entropy. *Journal of Optics A: Pure and Applied Optics*, *7*(1), 76-81. https://doi.org/10.1088/1464-4258/7/1/012

Buosciolo, A., Pesce, G., & Sasso, A. (2004). *New calibration method for position detector for simultaneous measurements of force constants and local viscosity in optical tweezers*. *230*, 357-368. https://doi.org/10.1016/j.optcom.2003.11.062

Ghislain, L. P., Switz, N. A., & Webb, W. W. (1994). Measurement of small forces using an optical trap. *Review of Scientific Instruments*, *65*(9), 2762-2768. https://doi.org/10.1063/1.1144613

Grier, D. G. (2003). A revolution in optical manipulation. *Nature*, *424*(6950), 810-816. https://doi.org/10.1038/nature01935

Michel, K. E. J., Pavel, Y., Eugene, M., Kouacou, M. A., & Zoueu, J. T. (2017). *Dynamics Study of the Deformation of Red Blood Cell by Optical Tweezers*, 59-69. https://doi.org/10.4236/ojbiphy.2017.72005

Neuman, K. C., Abbondanzieri, E. A., & Block, S. M. (2005). Measurement of the effective focal shift in an optical trap. *Optics Letters*, *30*(11), 1318. https://doi.org/10.1364/ol.30.001318

Osterman, N. (2010). TweezPal – Optical tweezers analysis and calibration software ☆. *Computer Physics Communications*, *181*(11), 1911-1916. https://doi.org/10.1016/j.cpc.2010.07.024

Rohrbach, A. (2005). Stiffness of optical traps: Quantitative agreement between experiment and electromagnetic theory. *Physical Review Letters*, *95*(16), 1-4. https://doi.org/10.1103/PhysRevLett.95.168102

Verdeny, I., Farré, A., Mas, J., López-Quesada, C., Martín-Badosa, E., & Montes-Usategui, M. (2011). Optical trapping: A review of essential concepts. *Optica Pura y Aplicada*, *44*(3), 527-551.

Yale, P., Edoukoua, K., Michel, J., Koffi, Y., & Kouacou, A. M. (2016). *Résumé. December 2017*.

Yale, P., Konin, J. E., & Kouacou, M. A. (2018). *New Detector Sensitivity Calibration and the Calculation of the Interaction Force between Particles Using an Optical Tweezer*. 1-11. https://doi.org/10.3390/mi9090425